Supporting Information

Thermite-Assisted Cu-Coated Al Powder as a Solid Propellant: Expanding the Utility of Coarse Al Powder

Soo-ho Jung[1,*], Jinhee Bae[1], Jihun Yu[1], Ho sung Kim[2], Soo hyung Kim[3]

[1] Nano Materials Research Division, Korea Institute of Materials Science, 797 Changwondaero, Seongsan-gu, Changwon, Gyeongnam 51508, Republic of Korea

[2] Research Center of Energy Convergence Technology, Pusan National University, Busandaehak-ro 63beon-gil, Geumjeong-gu, Busan, 46241, Republic of Korea

[3] Department of Nanoenergy Engineering, College of Nanoscience and Nanotechnology, Pusan National University, Busandaehak-ro 63beon-gil, Geumjeong-gu, Busan, 46241, Republic of Korea

***Corresponding author: Soo-ho Jung**

E-mail: chungleo@kims.re.kr

S1. Experimental Section

S1.1 Preparation of Cu-coated Al powders

To prepare the 300 mL copper coating solution, copper(II) sulfate pentahydrate (KANTO Chemical, extra pure) 12 g, EDTA (Junsei Chemical, extra pure) 16.5 g, 0.27 M formaldehyde solution (Samchun Chemical, 35.0 %), 3 g/L of H_3BO_3 (Samchun Chemical, 99.5 %) and 0.3 mg thiourea (Sigma-aldrich, reagent plus) were mixed using a magnetic stirrer at 250 rpm. After mixing, NaOH powder (Samchun Chemical, >98.0 %) was added to adjust the pH to a range between 12.5 and 13.

In the electroless plating bath, each chemical played a specific role in forming a uniform Cu coating. Copper(II) sulfate pentahydrate acted as the primary source of Cu^{2+} ions. EDTA served as a chelating agent to form stable complexes with Cu^{2+}, preventing the unwanted precipitation of copper hydroxide ($Cu(OH)_2$) in the highly alkaline environment and regulating the reduction rate for uniform deposition. Formaldehyde solution functioned as the primary reducing agent, reducing the Cu^{2+} ions to metallic Cu (Cu^0) on the Al powder surface. Boric acid was added as a buffer to stabilize the pH of the bath against local fluctuations during the intense reduction reaction, while NaOH was utilized to establish and maintain the highly alkaline conditions (pH 12 to 13) required to activate the reducing power of formaldehyde. Thiourea was added in a trace amount as a stabilizer to suppress the spontaneous decomposition of the bath. The overall reduction reaction can be expressed as follows:

$$Cu(EDTA)^{2-} + 2HCHO + 4OH^- \rightarrow Cu + 2HCOO^- + 2H_2O + H_2 + EDTA^{4-} \quad (S1)$$

The Cu coating was formed simply by immersing the NaOH-etched Al powder in the plating bath at room temperature under stirring, without any additional surface activation (e.g., with a Pd catalyst) or heating. Because the native oxide layer was removed by the NaOH etching, the exposed Al surface, which is electrochemically more active than Cu, initiated Cu nucleation, presumably through galvanic displacement between Al and the Cu^{2+} complexes. The deposited Cu nuclei then served as catalytic sites for the oxidation of formaldehyde, so that Cu^{2+} was further reduced on the Cu surface and a

continuous Cu layer grew autocatalytically. Accordingly, the Cu coating thickness can be controlled by the amount of Cu supplied relative to the total surface area of the Al powder and by the reaction time.

Aluminum powders (MK Metal, 99.5 %) with particle sizes (D_{50}) of 5 μm and 35 μm (20 g each) were pretreated in 100 mL of NaOH etching solution (pH 12 to 13) for 3 min to remove the native Al_2O_3 oxide layer from their surfaces. Subsequently, the etched powders were mixed with the prepared copper coating solution (300 mL for the 35 μm powder and 1 L of the solution with the same composition for the 5 μm powder, considering its larger specific surface area). The entire reaction was taken at room temperature. After 30 min of the reaction, the Cu-coated Al powders were recovered using a vacuum filtration system and dried overnight at 60 °C in a vacuum oven.

S1.2 Estimation of Cu content

The Cu content of the Cu/Al powders was estimated using a core–shell model, in which each particle was assumed to be a sphere with a diameter equal to its D_{50} value and covered with a uniform Cu shell of thickness t. The mass fraction of Cu (w_{Cu}) was calculated as

$$w_{Cu} = (\rho_{Cu}[(r+t)^3 - r^3])/(\rho_{Al} r^3 + \rho_{Cu}[(r+t)^3 - r^3]) \quad \text{(S2)}$$

where r is the radius of the Al core, and ρ_{Al} (2.70 g/cm³) and ρ_{Cu} (8.96 g/cm³) are the densities of Al and Cu, respectively. For the Cu/Al 5 μm powder, t was set to 100 nm based on the TEM observation (Figure 3), yielding a Cu content of ~29 wt%. This corresponds to ~8.3 g of Cu deposited on 20 g of the Al powder, i.e., ~80% of the Cu supplied by the plating bath (10.2 g of Cu in 1 L of the solution). Assuming that the same fraction of Cu was deposited on the 35 μm powder during the same reaction time (30 min), ~2.3 g of the 3.05 g of Cu in 300 mL of the solution was deposited, which corresponds to a Cu thickness of approximately 200 nm and a Cu content of ~10 wt%. The thin Al_2O_3 interlayer (~50 nm) observed by TEM was neglected, as it changed the calculated Cu content by less than 1 wt%.

S1.3 Characterization

X-ray diffraction (XRD, SmartLab XE, Rigaku) analysis was performed to confirm the successful coating process. The surface morphology and cross-sectional microstructure of the Cu-coated Al powders were observed using a scanning electron microscope (SEM, JSM-7001F, JEOL).

For more detailed characterization of the interface between the copper coating layer and the aluminum substrate, transmission electron microscopy (TEM, JEM-2200FS, JEOL) was conducted. The thermal properties of the powders were investigated using thermogravimetric analysis/differential scanning calorimetry (TGA/DSC, Discovery SDT 650, TA Instruments). The analysis was carried out under an air atmosphere with a heating rate of 10 °C/min. The mass of each sample was controlled at approximately 20 mg (ranging from 20.182 to 20.552 mg). The analyses were performed using a 90 μL alumina crucible under a gas flow rate of 100 mL/min, which is the standard setting for the instrument.

S1.4 Combustion and propulsion tests

For the ESD sensitivity, burn rate, and explosion pressure tests, a composite mixture of 1 μm Al, the sample powder, and WO_3 in a weight ratio of 15:15:70 was used. For the thrust test, the sample powder was mixed with KNSU (KNO_3:sucrose = 65:35 wt%) in a weight ratio of 10:90 (sample:KNSU).

The electrostatic discharge (ESD) sensitivity was evaluated using an ESD simulator (KES4021, Kikusui Electronics, Japan) equipped with a 330 pF capacitor, with a maximum charging voltage of 30 kV, corresponding to a maximum discharge energy of 149 mJ. Approximately 10 mg of each mixture was used for each test. A test was regarded as a “go” when ignition of the sample occurred upon discharge (as observed with a high-speed camera), and as a “no-go” otherwise. The ignition threshold was determined using a go/no-go-based bisection method. The first test was conducted at the maximum voltage (30 kV), and the voltage was halved for each subsequent test until a no-go result was obtained. Thereafter, each test was conducted at the midpoint between the lowest go voltage and the highest no-go voltage, and this procedure was repeated to narrow the interval between them. The

threshold voltage (V) thus obtained was converted into the threshold energy (E) using $E = \frac{1}{2}CV^2$, where C is the capacitance. The burn rate was measured using the apparatus shown in Figure S1, with approximately 870 mg of each mixture.

The explosion pressure was measured in a sealed stainless-steel vessel with an internal volume of ~9 mL. Approximately 15 mg of each mixture was loaded into the vessel and ignited by a hot wire (~2 A, ~4 V). The pressure was measured using a piezoelectric pressure sensor (113B28, PCB Piezotronics, USA) connected to a signal conditioner (480C02, PCB Piezotronics, USA), and the signal was recorded using a digital oscilloscope (TDS 2012B, Tektronix, USA). The maximum pressure and the pressurization rate were obtained from the pressure–time curves.

The thrust was measured using a small rocket motor (Figure S1) mounted on a load cell (PW2DC3MR, capacity: 72 kg). Approximately 7.66 g of the propellant was loaded into the motor. The load data (kg) recorded by the load cell were converted into thrust (N), and the total impulse (I_t) was obtained by integrating the thrust–time curve. The specific impulse (I_{sp}) was calculated as $I_{sp} = I_t/(m_p \cdot g_0)$, where m_p is the propellant mass and g_0 is the standard gravitational acceleration (9.81 m/s^2).

All tests were repeated five times, and the results are presented as the mean ± standard deviation.

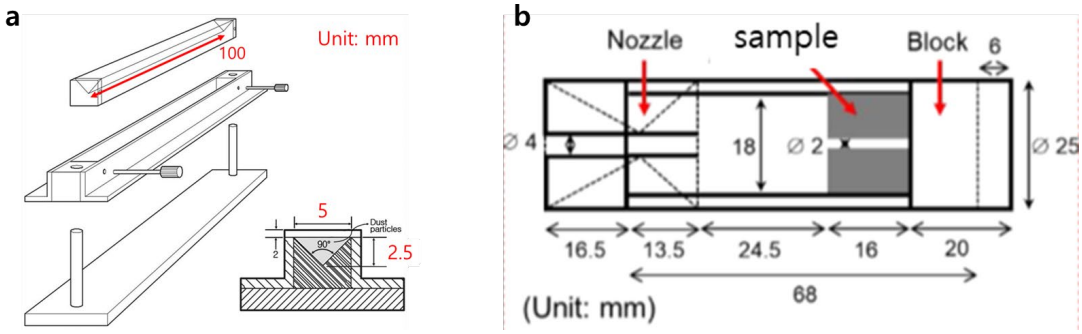


Figure S1. Schematics of the cells for combustion and propulsion tests. a) burn rate test, b) thrust test.

S2. Particle size distributions, microstructures, and TGA/DSC results of the control samples

To examine whether the enhanced heat release of the Cu/Al powders originates from the NaOH etching itself, NaOH-etched Al powders without Cu coating were prepared as control samples. For the etched control samples, the Al powders were etched in a NaOH solution (pH 13) for 3 min under magnetic stirring at 250 rpm, and the recovered powders were dried in a drying oven at 60 °C.

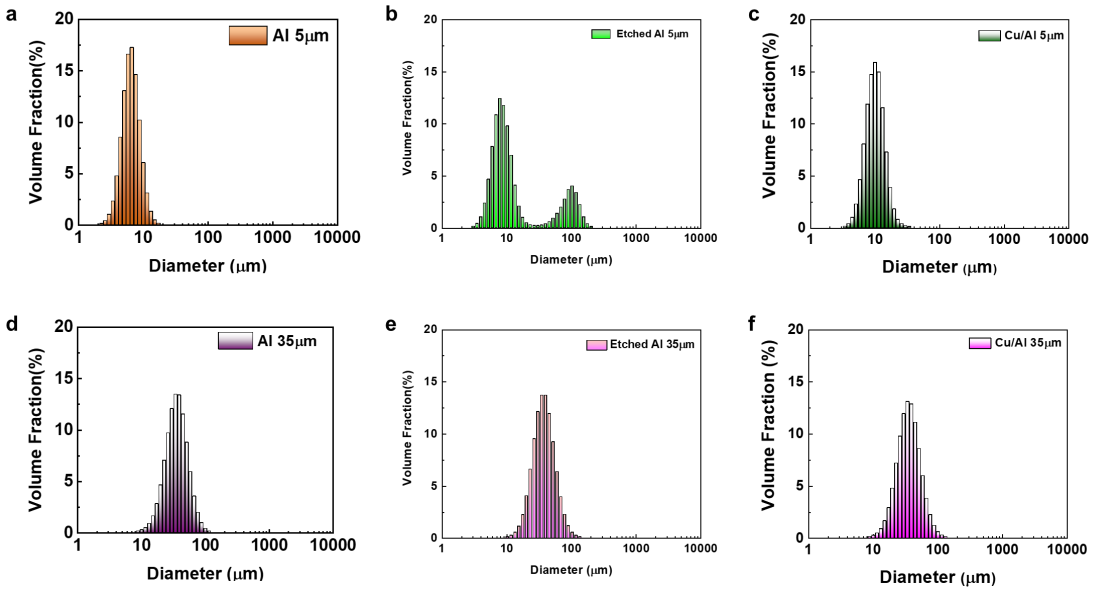


Figure S2. Particle size distributions of the pristine, NaOH-etched, and Cu-coated Al powders: a–c) 5 μm powders and d–f) 35 μm powders.

As shown in Figure S2 and Table S1, the etched Al 5 μm powder exhibited a bimodal size distribution with a second peak at ~100 μm and an increased D_{50} (8.65 μm, compared with 6.02 μm for the pristine powder). This indicates severe agglomeration of the fine particles during the dissolution and regrowth of the surface oxide layer. In contrast, no agglomeration was observed for the etched Al 35 μm powder, and its D_{10}, D_{50}, and D_{90} increased only slightly, by ~1 μm. After Cu coating, the large agglomerates observed for the etched powder were no longer present. The D_{50} of the Cu/Al 5 μm

powder (9.35 μm) was larger than that of the pristine powder, whereas the change in the particle size of the Cu/Al 35 μm powder was within the measurement error.

Table S1. Particle size distributions of the pristine, NaOH-etched, and Cu-coated Al powders

Powder size distribution (μm)	D_{10}	D_{50}	D_{90}
Al 5 μm	3.99	6.02	9.04
Etched Al 5 μm	5.24	8.65	92.35
Cu/Al 5 μm	6.02	9.35	14.40
Al 35 μm	19.37	33.16	55.16
Etched Al 35 μm	20.58	34.13	56.94
Cu/Al 35 μm	19.26	33.15	56.71

The NaOH etching alone did not improve the heat release of the Al powder. As shown in Figure S3, both the weight gain and the heat release of the etched Al 5 μm powder (2077.7 J/g) were considerably lower than those of the pristine powder (6969 J/g). The weight loss of ~3% below ~400 °C for the etched powder indicates the dehydration of the hydrated oxide (hydroxide) layer formed on the etched surface during etching and drying. This regrown oxide layer, together with the agglomeration of the particles, is considered to suppress the oxidation of the Al core. These results confirm that simply removing the native oxide layer does not enhance the heat release. Since the Cu/Al powders were prepared from the same etched powders, the enhanced heat release of the Cu/Al powders can be attributed to the Cu coating rather than to the etching process.

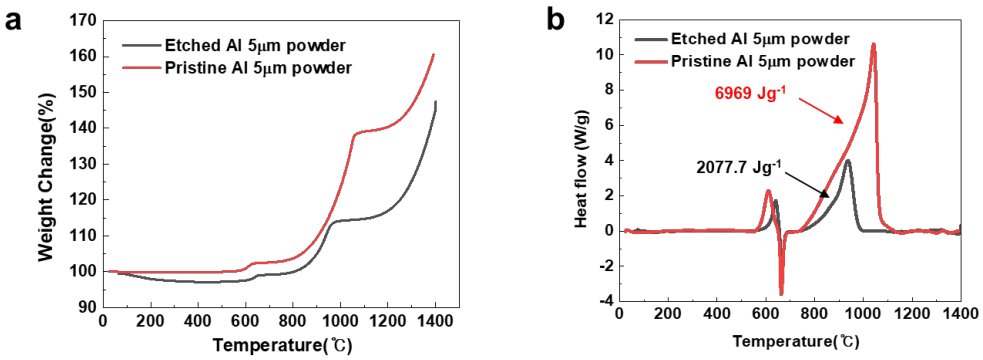


Figure S3. a) TGA and b) DSC curves of the pristine and NaOH-etched Al 5 μm powders.

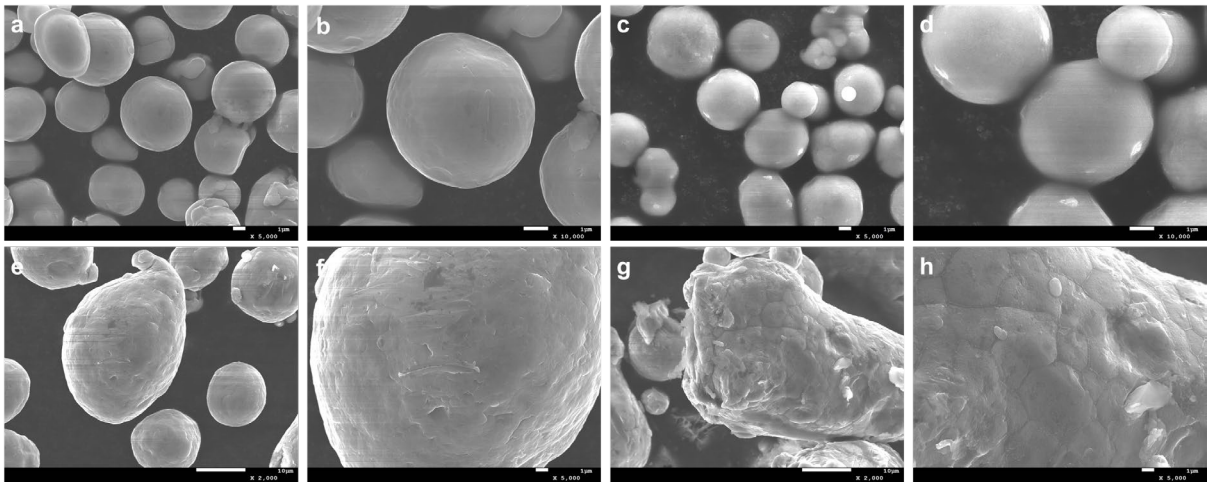


Figure S4. SEM images of the pristine and NaOH-etched Al powders: a, b) pristine Al 5 μm, c, d) etched Al 5 μm, e, f) pristine Al 35 μm, and g, h) etched Al 35 μm powders.

S3. d-spacings of the SAED and FFT patterns in Figure 3

Table S2. Measured d-spacings of the SAED and FFT patterns in Figure 3.

	(hkl)	Measured d-spacing (Å)	Theoretical d-spacing (Å)	Percent Error (%)
Figure 3b inset (Al SAED)	**(200)**	**1.744**	**2.024**	**13.83**
Figure 3b inset (Al SAED)	**(220)**	**1.362**	**1.4310**	**4.82**
Figure 3d inset (Cu FFT)	**(111)**	**1.926**	**2.0880**	**7.76**
Figure 3d inset (Cu FFT)	**(200)**	**1.758**	**1.8080**	**2.77**

※ Theoretical d-spacings were taken from PDF #04-0787 (Al) and PDF #04-0836 (Cu).